PI3Kδ inhibitor YY-20394 is effective alone or in combination with Bcl-2 inhibitor ABT199 in acute myeloid leukemia cells

YINGHUA GENG[1], LILI ZHOU[1], YAN LOU[1], JIAQI CHEN[1], QI LIU[1], JI SHEN[1], YANLI YANG[1] and WENJUAN WU[2]

[1]Department of Hematology, The First Affiliated Hospital of Bengbu Medical University, Bengbu, Anhui 233000, P.R. China; [2]Department of Biochemistry and Molecular Biology, Bengbu Medical University, Bengbu, Anhui 233030, P.R. China

Received November 19, 2025; Accepted May 28, 2026

DOI: 10.3892/or.2026.9153

Abstract. YY-20394 (linperlisib), a highly specific PI3Kδ inhibitor, has demonstrated promising efficacy in a variety of hematological malignancies in clinical trials. ABT199 (venetoclax) as a monotherapy shows limited effects in acute myeloid leukemia (AML), underscoring the need for novel combinatorial therapeutic strategies. The drug sensitivity and potential synergistic effects of YY-20394 and ABT199 were evaluated in three AML cell lines, MV-4-11, U937 and THP-1, using a Cell Counting Kit-8 assay. Apoptosis and cell cycle distribution were assessed using dual acridine orange/ethidium bromide staining and flow cytometry. Reverse transcription-quantitative PCR and western blot analyses were employed to quantify the levels of Bcl-2 apoptotic family members, c-Myc, Akt and ERK. YY-20394 inhibited the viability of MV-4-11, U937 and THP-1 cells in a concentration-dependent manner. In U937 cells, the highest IC_{50} value was observed, and YY-20394 effectively suppressed their proliferation, induced apoptosis and caused cell cycle arrest. Furthermore, the combination of YY-20394 and ABT199 demonstrated a synergistic effect in MV-4-11 cells, significantly enhancing apoptosis compared with either agent alone. Compared with the negative control group, the levels of c-Myc and Akt phosphorylation were significantly reduced in the YY-20394 group, and their inhibitory effects were retained in the combination group. ERK phosphorylation was significantly increased in the combination group. However, alterations in the Bcl-2 pathways did not show a pattern consistent with the observed apoptotic phenotype. In summary, YY-20394 is effective for inhibiting proliferation of AML cells, and its combination with ABT199 has synergistic pro-apoptotic effects in MV-4-11 cells, which provides new insights and potential avenues for the treatment of AML and its subtypes. Further studies are warranted to explore the therapeutic efficacy and underlying molecular mechanisms of this combination in additional AML subtypes.

Correspondence to: Professor Yanli Yang, Department of Hematology, The First Affiliated Hospital of Bengbu Medical University, 287 Changhuai Road, Bengbu, Anhui 233000, P.R. China
E-mail: yanli_y@126.com

Professor Wenjuan Wu, Department of Biochemistry and Molecular Biology, Bengbu Medical University, 2,600 Donghai Road, Bengbu, Anhui 233030, P.R. China
E-mail: 2

Key words: acute myeloid leukemia, linperlisib, venetoclax, combination therapy, FMS-like tyrosine kinase 3-internal tandem duplications

Introduction

Acute myeloid leukemia (AML) is a hematological malignancy characterized by the clonal expansion and differentiation blockade of myeloid progenitor cells (1). The incidence of AML is age-dependent, and a 5-year relative survival rate among patients in the United States is only 30.5% (1,2). Although most patients with AML receive induction and consolidation chemotherapy, 20-50% eventually develop chemoresistance (3). Furthermore, the high relapse rate of AML leads to poor prognosis and low remission rates (4). Targeted therapies have shown efficacy in these refractory or relapsed patients (5). Due to the high heterogeneity of AML, identifying new targeted small-molecule inhibitors remains critical (6).

Previous studies have shown that the PI3K-Akt pathway is aberrantly activated in 50-80% of patients with AML and serves a pivotal role in leukemic cell proliferation (6,7). PI3Kδ, a member of the Class I PI3K family, is highly expressed in leukocytes (8). Several PI3Kδ inhibitors have demonstrated anti-proliferative and pro-apoptotic effects in AML cells (9,10). YY-20394 (linperlisib) is an oral and highly selective PI3Kδ inhibitor with less activity against PI3Kγ, giving a kinase inhibition profile that is nearly two orders of magnitude more selective for PI3Kδ, which may improve tolerability compared with other PI3K inhibitors (11). In clinical studies, YY-20394 has shown promising results in hematologic malignancies, including peripheral T-cell lymphoma, B-cell lymphoma and follicular lymphoma, with an overall response rate exceeding 60% and a manageable safety profile (11-13). However, the effects of YY-20394 in AML remains unclear.

ABT199 (venetoclax), a Bcl-2 inhibitor, has been approved in combination with hypomethylating agents or low-dose cytarabine for newly diagnosed patients with AML who are

elderly or unfit for intensive chemotherapy (14). Nevertheless, resistance to ABT199 has been observed in a subset of patients with AML (15). For example, FMS-like tyrosine kinase 3 (FLT3)-internal tandem duplications (ITDs) mutation could increase the expression of anti-apoptotic Bcl-2 family proteins and is often associated with AML resistance to ABT199 (16). Research has suggested that targeting the PI3K/Akt pathway may enhance the efficacy of ABT199 in AML (17). In the present study, the sensitivity of different AML cell lines to YY-20394 and ABT199 was investigated. Furthermore, the effects of YY-20394 alone and in combination with ABT199 on AML cells were assessed, providing new insights for the treatment of AML.

Materials and methods

Cell culture. Three AML cell lines, MV-4-11 (human leukemia cells; cat. no. CL-0572), U937 (human monocytic leukemia cells; cat. no. CL-0239) and THP-1 (human histiocytic lymphoma cells; cat. no. CL-0233), and their corresponding cell-specific media were purchased from Procell Life Science & Technology Co., Ltd. All cells were authenticated by short tandem repeat profiling and grown at 37˚C under 5% CO_2 and 95% relative humidity. For U937 cells, 5 and 10 μM YY-20394 were used for treatment. For MV-4-11 cells, treatments included 120 nM YY-20394, 30 nM ABT199 and a combination of 120 nM YY-20394 with 30 nM ABT199. The negative control (NC) group received an equal volume of drug-free culture medium.

Half-maximal inhibitory concentration (IC_{50}) determined by cell counting Kit-8 (CCK-8) assay. A CCK-8 assay was performed using the Cell Counting Kit-8 (APeXBIO Technology LLC). A total of 100 μl cell suspension was spread into a 96-well plate ($1.5x10^4$ cells per well) and incubated at 37˚C in a 5% CO_2 environment. The cells were divided into two groups: The experimental group (As), which received the drug (YY-20394 or ABT199), and the control group (Ac), which received no drug. Additionally, a blank group (Ab), consisting only of culture medium, was included. Following previous studies for reference, the concentration gradients for the drugs were as follows: For YY-20394 (18), the concentrations used in MV4-11 cells were 10, 50, 100, 500, 1,000 and 5,000 nM; in THP-1 cells, they were 500, 1,000, 2,000, 5,000, $1x10^4$ and $2x10^4$ nM; and in U937 cells, the concentrations were 1,000, 5,000, $1x10^4$, $2x10^4$, $5x10^4$ and $1x10^5$ nM. For ABT199, the concentrations used in MV4-11 cells were 5, 25, 100, 200, 300, 400 and 600 nM (19,20); in THP-1 cells, the concentrations used were 1,000, $1x10^4$, $2x10^4$, $3x10^4$, $4x10^4$ and $5x10^4$ nM (21); and in U937, they were 1,000, 5,000, 8,000, $1x10^4$, $1.5x10^4$, $2x10^4$ and $4x10^4$ nM.

Following cell adherence to the plate, the diluted drugs were incubated with the cells for either 24 or 48 h. Subsequently, 10 μl CCK-8 solution was added to each well and incubated for 4 h. The optical density (OD) value at λ=450 nm was measured using a plate reader. The percentage of cell growth inhibition was calculated using the following formula: Cell growth inhibition (%)=1-[(As-Ab)/(Ac-Ab)] x100%. The IC_{50} value of the drug was determined through linear regression analysis. Specifically, drug concentrations were transformed to their logarithmic (log) values, and the IC_{50} values were calculated using the 'log(inhibitor) vs. normalized response-variable slope' model in GraphPad software (version 8; Dotmatics). Growth inhibition curves were also plotted based on this analysis.

Combination index (CI) value detected by CCK-8 assay. The experimental groups were divided into the YY-20394, ABT199 and YY-20394+ABT199 combination groups. The drug concentration was a multiple of the IC_{50} value (1, 0.5, 0.25, 0.125, 0.0625 and 0.03125 times). Cell growth inhibition was measured using a CCK-8 assay as described. Subsequently, CI values were calculated using CompuSyn software (version 1.0; ComboSyn, Inc.), and Fa-CI plots of equivalent dose-effect ratios were drawn based on the obtained data. The strength of drug-drug interactions in the combination of YY-20394 and ABT199 could be quantitatively determined by the magnitude of the CI values: CI >1 was antagonistic, CI=1 was additive, 0.7< CI <1 was weakly synergistic, 0.3< CI <0.7 was synergistic and CI <0.3 was strongly synergistic.

Determining apoptosis by the dual acridine orange/ethidium bromide (AO/EB) staining. According to the instructions, cell apoptosis was detected using dual AO/EB staining using a normal/apoptotic/necrotic cell detection kit (Jiangsu KeyGen Biotech Co., Ltd.). The results were observed under a fluorescence microscope at 510 nm. According to the cell morphology and staining results, the following four types of cells were counted (the total number of cells >200): i) Normal cells were defined as round cells with uniformly green-stained nucleoplasm and consistent size and shape; ii) necrotic cells were ellipsoidal with uniformly orange-yellow-stained nucleoplasm and consistent size and shape; iii) early apoptotic cells were indicated by green nucleoplasm and cells exhibiting irregular shapes, such as crescent-like morphology; and iv) late apoptotic cells where the nucleoplasm was orange, chromatin was condensed, the nucleus was fragmented into punctate structures of varying sizes and cytoplasmic blebbing was observed. Apoptosis rate=(early apoptotic cells + late apoptotic cells)/total number of cells x100%. Cell necrosis rate=necrotic cells/total number of cells x100%.

Cell cycle assay. Drug-exposed cells were washed with PBS and fixed homogeneously in pre-cooled 95% ethanol at 4˚C overnight. After washing with PBS, the cells were stained with propidium iodide (PI) solution (Beijing Solarbio Science & Technology Co., Ltd.) containing RNase A and incubated in the dark at 37˚C for 30 min. The cell cycle distribution was analyzed using a flow cytometer (NovoCyte; Agilent Biosciences). Flow cytometry data were analyzed using FlowJo software (BD Biosciences). Briefly, target cell populations were first gated based on forward scatter (FSC) and side scatter (SSC) parameters to exclude debris and non-viable fragments. Doublets and cell aggregates were subsequently excluded by gating on FSC-A vs. FSC-H. Cell cycle distribution was then determined based on DNA content in the PE channel. To ensure analytical accuracy and consistency across groups, a gating template was established from NC group and subsequently applied to all other experimental groups.

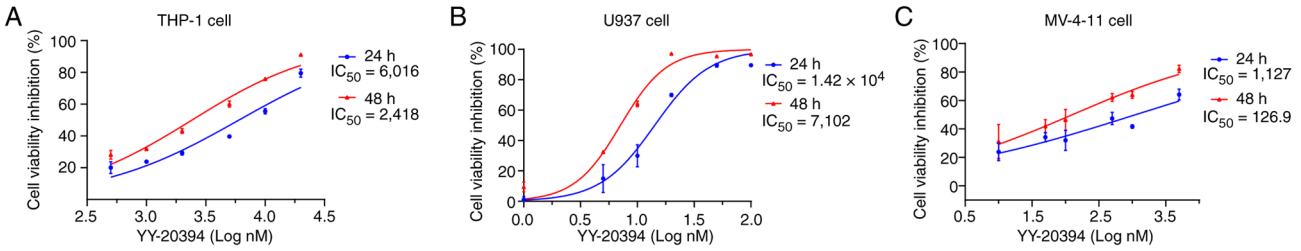

Figure 1. Three acute myeloid leukemia lines exhibit different sensitivities to YY-20394. The dose-response curves indicate the percentage growth inhibition of each cell line in response to increasing concentrations of YY-20394 for 24 or 48 h, as measured using Cell Counting Kit-8 assays. (A) THP-1 cells were treated with YY-20394 (500-20,000 nM). (B) U937 cells treated with YY-20394 (1,000-10,0000 nM). (C) MV-4-11 cells were treated with YY-20394 (10-5,000 nM). Data are presented as mean ± SD from three independent experiments. IC_{50}, half-maximal inhibitory concentration.

Reverse transcription-quantitative PCR (RT-qPCR). The mRNA levels of Akt, mTOR, myeloid cell leukemia-1 (Mcl-1), Bcl-2 interacting mediator of cell death (Bim), Bcl-2, B-cell lymphoma-extra large (Bcl-xL), Bcl-2 antagonist killer 1 (Bak) and Bcl-2 associated X (Bax) were assessed using RT-qPCR in drug-exposed cells. GAPDH was used as an internal reference gene. Specific primers are presented in Table SI. Total RNA was extracted from cell samples using TRIzol reagent (Tiangen Biotech Co., Ltd.), and cDNA was synthesized using the FastQuant cDNA First Strand Synthesis Kit (Tiangen Biotech Co., Ltd.). The PCR reaction mixture was prepared by combining SuperReal PreMix Plus (SYBR Green; Tiangen Biotech Co., Ltd.) and specific primers, following the manufacturer's instructions. The PCR amplification protocol was as follows: 95˚C for 15 min, followed by 40 cycles of 95˚C for 10 sec, 55˚C for 30 sec and 72˚C for 32 sec. A final extension step was performed at 95˚C for 15 sec, 60˚C for 60 sec and 95˚C for 15 sec. The amplification results were detected using an ABI 7300 fluorescence quantitative PCR instrument (Applied Biosystems; Thermo Fisher Scientific, Inc.), and relative gene expression was analyzed using the $2^{-\Delta\Delta Cq}$ method (22).

Western blot analysis. The protein levels of Akt (Akt Polyclonal Antibody; 1:1,000; ImmunoWay Biotechnology Company; cat. no. YT0185), phosphorylated (p)-Akt [Akt (phospho Ser473) Polyclonal Antibody; 1:1,000; ImmunoWay Biotechnology Company; cat. no. YP0006), ERK (Mouse Anti-ERK1/2 antibody; 1:1,000; BIOSS; cat. no. bsm-33337M), p-ERK [Phospho-ERK1/2 (Thr202/Tyr204) Antibody; 1:1,000; Affinity Biosciences; cat. no. AF1015), Mcl-1 [MCL1 Rabbit mAb (hp7u); 1:1,000; Nature Biosciences; cat. no. A57858], Bim [Bim Rabbit mAb (7kqv); 1:1,000; Nature Biosciences; cat. no. A83449], Bcl-2 (Rabbit Anti-Bcl-2 antibody; 1:1,000; BIOSS; cat. no. bs-0032R), Bcl-xL [Bcl-xL Rabbit mAb (kn97); 1:1,000; Nature Biosciences; cat. no. A66923], Bak [Bak Rabbit mAb (RX7I); 1:1,000; Nature Biosciences; cat. no. A53931], Bax (Rabbit Anti-Bax antibody; 1:1,000; BIOSS; cat. no. bs-0127R) and c-Myc [c-Myc Rabbit mAb (paYu); 1:1,000; Nature Biosciences; cat. no. A23647] were assessed using western blot in drug-exposed cells. Actin (1:3,000; BIOSS; cat. no. bs-0061R) was used as an internal reference.

RIPA lysis buffer (Beyotime Biotechnology) was added to the cell samples, and proteins were extracted by ultrasound homogenization on ice. Protein concentration was determined using the BCA protein assay (Beijing Solarbio Science & Technology Co., Ltd.) and adjusted to 1.5 mg/ml (~21 μg/lane). Proteins were separated on 5 and 10% polyacrylamide gels and then transferred to activated PVDF membranes. A color-pre-stained protein marker (10-180 kDa; Biodragon) was used to indicate the molecular weight of the target protein. The membrane was blocked with 5% bovine serum albumin (Wuhan Servicebio Technology Co., Ltd.) at room temperature for 1 h. The membrane was then incubated overnight at 4˚C with the primary antibody specific to the target protein. Subsequently, the membrane was incubated with the corresponding secondary antibody (1:5,000; Nature Biosciences; Goat Anti-Mouse, cat. no. M00001; Goat Anti-Rabbit, cat. no. R00001) at room temperature for 1 h, and the results were detected using an ECL reagent kit (Harbin HaiGene Biotech Co., Ltd.) through chemiluminescence.

Statistical analysis. One-way analysis of variance followed by Tukey's post hoc test was performed using GraphPad Prism for multiple group comparisons. All pairwise comparisons were two-tailed. All data are presented as the mean ± standard deviation. A P-value of <0.05 was considered to indicate a statistically significant difference.

Results

Differential sensitivity of YY-20394 in different AML cell lines. The IC_{50} values of YY-20394 were evaluated to assess the sensitivity in different AML cell lines. In THP-1 cells, the 24 and 48 h IC_{50} values of YY-20394 were 6,020 and 2,420 nM, respectively (Fig. 1A). In U937 cells, the 24 and 48 h IC_{50} values of YY-20394 were $1.42x10^4$ and 7,102 nM, respectively (Fig. 1B). The 24 and 48 h IC_{50} values of YY-20394 in MV-4-11 cells were 1,127 and 126.9 nM, respectively (Fig. 1C). Comparatively, MV-4-11 cells were more sensitive to YY-20394, while THP-1 and U937 cells were less sensitive. YY-20394 exhibited a smoother dose-response profile in U937 cells, which were selected for further experiments.

YY-20394 inhibits U937 cell proliferation, promotes apoptosis and arrests the G_1/S phase. Cell apoptosis and the cell cycle are important biological processes that collectively determine the proliferation and survival of malignant cells. The dual AO/EB assay revealed that YY-20394 significantly induced apoptosis in U937 cells (P<0.001), with the apoptosis rate being significantly higher in the 10 μM group compared with the 5 μM group (P<0.0001) (Fig. 2A and B). Flow cytometry analysis

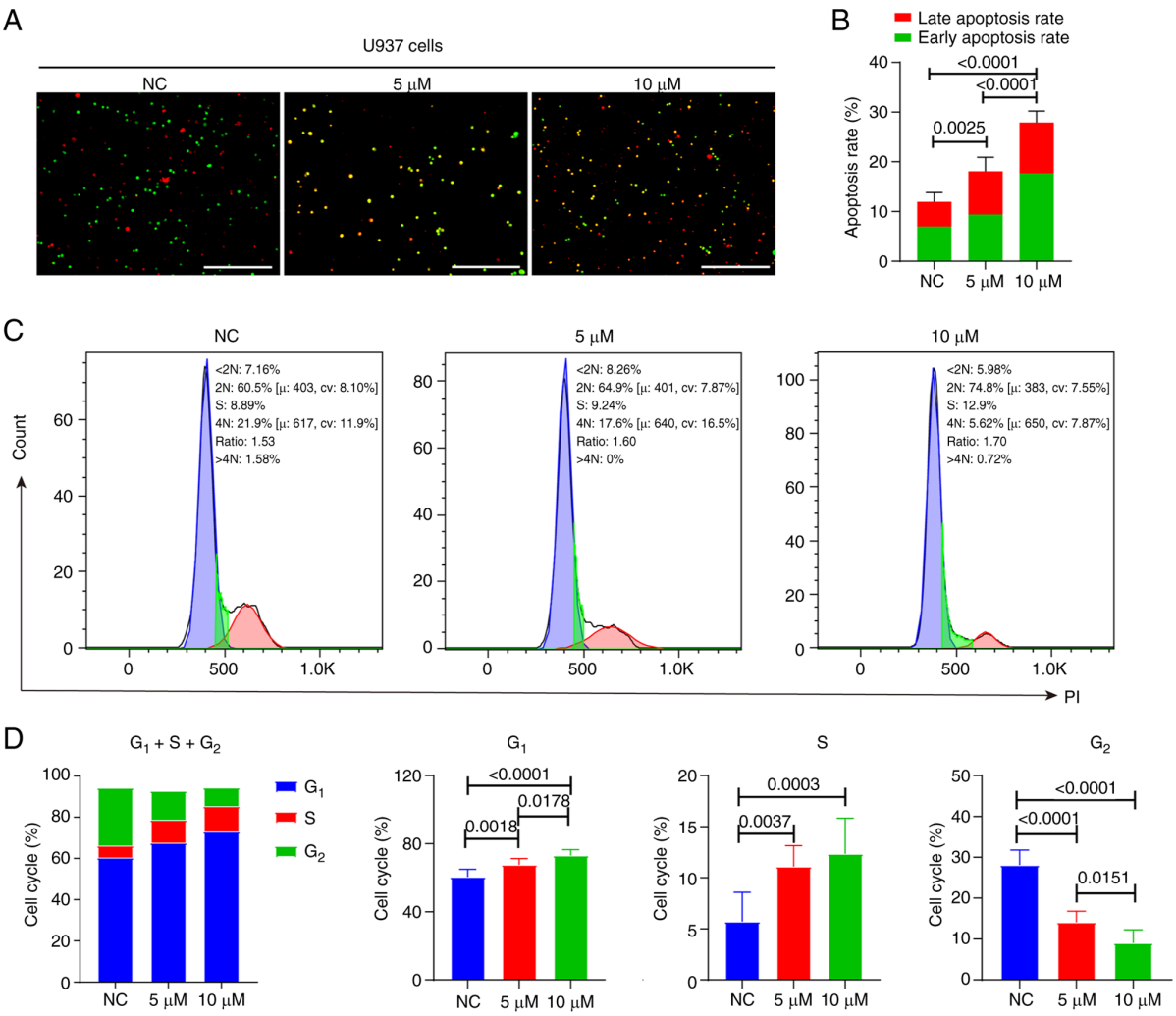

Figure 2. YY-20394 could influence the apoptosis and cell cycle in U937 cells. (A) U937 cells were treated with 5 and 10 μM of YY-20394 for 48 h. Early and late apoptotic cells were stained using the acridine orange/ethidium bromide dual staining method, and apoptosis was assessed based on the color and morphology of the cells. Magnification, x100; scale bar, 100 μm. (B) Quantification of total apoptotic cells. (C) Cell cycle distribution (G_1, S and G_2 phases) was analyzed using flow cytometry after PI staining. (D) Differences in cell cycle phase distribution were compared using statistical analysis and presented as bar charts. Data are presented as mean ± SD from three independent experiments. PI, propidium iodide; NC, negative control.

was used to assess the effects of YY-20394 on the cell cycle (Fig. 2C and D). Compared with the NC group, treatment with 5 and 10 μM of YY-20394 significantly increased the proportion of cells in the G_1 and S phases ($P<0.01$) while significantly reducing the population in the G_2 phase ($P<0.0001$), indicating that YY-20394 interfered with cell cycle progression at the G_1/S transition and early S phase. Overall, YY-20394 could inhibit U937 cell proliferation, promote apoptosis and induce arrest at G_1/S transition and in early S phase.

YY-20394 and ABT199 have a synergistic effect in MV-4-11 cells. The percentage of cell proliferation inhibition of ABT199 was assessed to determine its sensitivity in different AML cell lines (Fig. 3A-C). The results revealed that the IC_{50} values of ABT199 were $2.06x10^4$, $1.36x10^4$ and 161.80 nM for 24 h in THP-1, U937 and MV-4-11 cells, respectively, and $1.17x10^4$, $7.90x10^3$ and 30.47 nM for 48 h, respectively. To assess the potential synergistic effect of YY-20394 and ABT-199, three AML cell lines were treated with a range of doses based on the respective IC_{50} values of each drug. No significant synergistic effect was observed in THP-1 cells (CI>1, Fig. 3D), and only a negligible synergistic effect was detected in U937 cells (CI=0.895, Fig. 3E). Notably, synergistic interactions were observed in MV-4-11 cells, with the CI value of the optimal dose combination being 0.17 (Fig. 3F). Based on these results, the concentration with the strongest synergistic effect was selected for further experiments with MV-4-11 cells.

YY-20394 and ABT199 synergistically promote apoptosis in MV-4-11 cells without inducing cell cycle arrest. Dual AO/EB staining indicated that YY-20394 and ABT199 alone significantly promoted apoptosis in MV-4-11 cells compared with the NC group ($P<0.001$) (Fig. 4A and B). Moreover, the combination of the two drugs exhibited a higher apoptosis rate than either drug alone. Flow cytometry analysis further revealed that ABT199 significantly reduced the S phase in MV-4-11 cells ($P=0.0006$), with YY-20394 showing a similar trend ($P=0.0510$) (Fig. 4C and D). By contrast, there were no significant differences in G_1 and G_2 phases between the two drugs alone, in combination or compared with the NC group (all $P>0.05$). These findings suggest that YY-20394 and ABT199 may influence DNA replication in MV-4-11 cells.

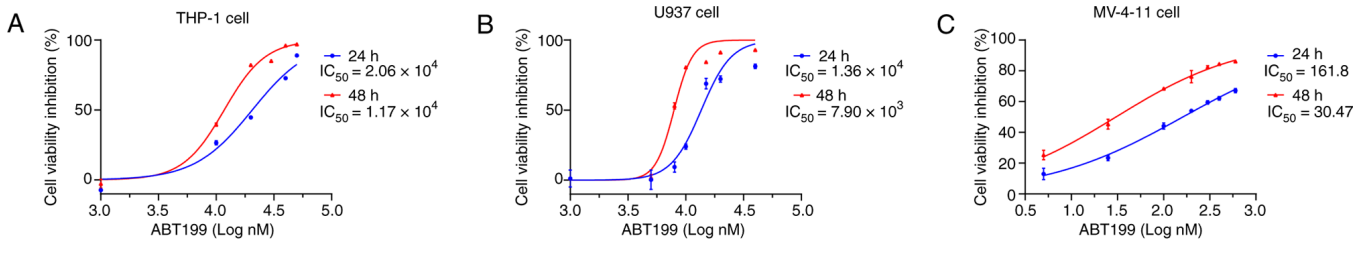

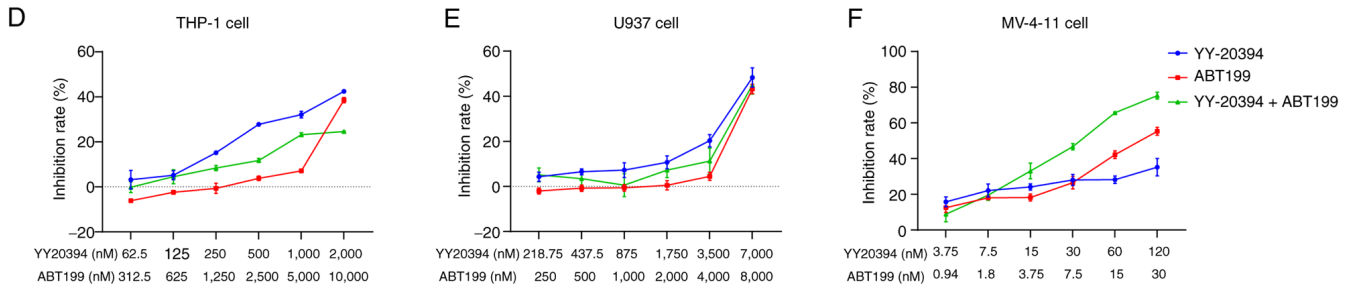

YY20394 (nM)	ABT199 (nM)	Fa	CI
62.5	312.5	0.0086	4.883
125	625	0.0449	1.741
250	1,250	0.0834	1.814
500	2,500	0.1172	2.519
1,000	5,000	0.2352	2.299
2,000	10,000	0.2456	4.367

YY20394 (nM)	ABT199 (nM)	Fa	CI
218.75	250	0.0387	0.895
437.5	500	0.0533	1.218
875	1,000	0.0635	1.975
1,750	2,000	0.0912	2.566
3,500	4,000	0.1453	2.958
7,000	8,000	0.4499	1.515

YY20394 (nM)	ABT199 (nM)	Fa	CI
3.75	0.94	0.09	19.764
7.5	1.8	0.2	11.269
15	3.75	0.33	0.592
30	7.5	0.47	0.357
60	15	0.66	0.178
120	30	0.75	0.170

Figure 3. Combination of YY-20394 and ABT199 has a synergistic effect on MV-4-11 cells. The dose-response curves indicate the percentage growth inhibition of (A) THP-1, (B) U937 and (C) MV-4-11 cells in response to increasing concentrations of ABT199 for 24 or 48 h, as measured using CCK-8 assays. (D) THP-1, (E) U937 and (F) MV-4-11 cells were treated with YY-20394, ABT199 alone or YY-20394/ABT199 combination at a constant ratio relative to the IC_{50} value for 48 h. Cell inhibition was assessed using the CCK-8 assay, and CI values were calculated to evaluate the effects of YY-20394 and ABT199 in three acute myeloid leukemia cell lines. Data are presented as mean ± SD from three independent experiments. CCK-8, Cell Counting Kit-8; IC_{50}, half-maximal inhibitory concentration; Fa, fraction affected; CI, combination index.

YY-20394 and ABT199 synergistically induce MV-4-11 cell apoptosis, which may be associated with c-Myc. ABT199 specifically targets Bcl-2. Mcl-1 and Bcl-2 could inhibit apoptosis by binding to the BH3-specific protein Bim, thereby preventing Bim from activating Bax and Bak (23). Whether YY-20394 and ABT199 synergistically promote apoptosis via the Bcl-2 pathway was investigated (Fig. 5A-E). The results revealed changes in the levels of anti-apoptotic proteins Mcl-1, Bcl-2 and Bcl-xL that were inconsistent with the observed apoptotic phenotype in MV-4-11 cells (Fig. 5A, C and D). Specifically, Mcl-1 transcription (P=0.001) and protein (P=0.0783) levels were increased in YY-20394 alone compared with the NC group. Mcl-1 transcription levels decreased while protein levels increased in the combination group compared with either agent alone. Furthermore, no inhibitory effects on Bcl-2 or Bcl-xL were observed at transcription level with ABT199 alone or in combination (all P>0.05) (Fig. 5B), while significant upregulations were observed in protein levels (P<0.05) (Fig. 5E). Bim and Bak transcription levels increased while protein levels decreased in the YY-20394 group compared with the NC group. Additionally, levels of pro-apoptotic factors Bim, Bak and Bax decreased in the combination group compared with NC or ABT199 alone, which contrasts with the observed pro-apoptotic phenotype (Fig. 5C-E).

Due to the critical role of c-Myc in cancer cell survival and apoptosis regulation (24), the protein levels of c-Myc were evaluated. The results demonstrated that the combination treatment significantly reduced c-Myc protein levels compared with the NC (P=0.001) and ABT199 alone (P=0.0007) (Fig. 5F and G). Therefore, the synergistic pro-apoptotic effects of the combined treatment may be associated with c-Myc suppression.

Synergistic effect of YY-20394 and ABT199 in MV-4-11 cells is associated with inhibition of p-Akt and increase of p-ERK. Previous studies have suggested that the effects of PI3Kδ inhibitors on tumor cell proliferation or apoptotic signaling may be mediated through the regulation of PI3K/Akt and ERK pathways (25,26). Whether the synergistic effects of YY-20394 and ABT199 on MV-4-11 cells are associated with these pathways was investigated (Fig. 6A). Compared with the NC, p-Akt levels were reduced in both the YY-20394 alone (P=0.0074) and in combination (P=0.0149) (Fig. 6B-D). By contrast, p-ERK levels increased in the ABT199 alone and in combination compared to the NC (P=0.0253). Additionally, the p-ERK/ERK ratio was higher in the combination group than in the ABT199 alone (P=0.0291) (Fig. 6E-G).

Discussion

PI3K inhibitors have demonstrated limited clinical success due to the adverse effects of inhibiting other isoforms, highlighting the need to develop subtype-specific PI3K inhibitors (27). PI3Kδ is commonly expressed in most AML cells (21),

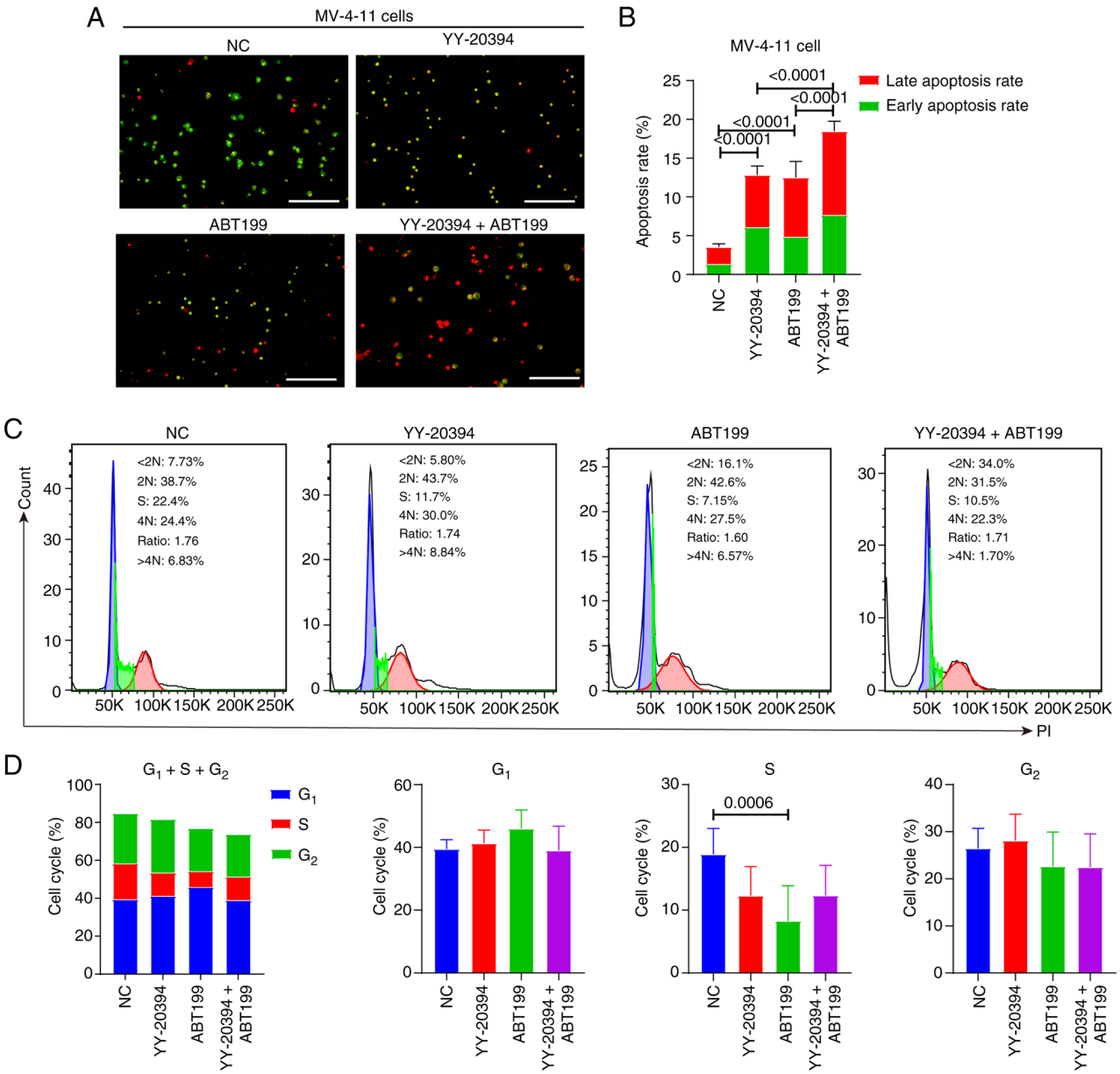

Figure 4. YY-20394 and ABT199 synergistically promote apoptosis in MV-4-11 cells without inducing cell cycle arrest. MV-4-11 cells were treated with 120 nM of ABT199, 30 nM of YY-20394 or a combination of both for 48 h. (A) Early and late apoptotic cells were assayed using the acridine orange/ethidium bromide dual staining method. Magnification, x400; scale bar, 20 μm. (B) Quantification of total apoptotic cells. (C) Cell cycle distribution (G_1, S and G_2 phases) was analyzed using flow cytometry after PI staining and (D) the statistical results were presented as bar charts. Data are presented as mean ± SD from three independent experiments. PI, propidium iodide; NC, negative control.

making it a therapeutically relevant target. YY-20394, a highly selective PI3Kδ inhibitor, has demonstrated efficacy in various hematologic malignancies (28). However, its role in AML remains unclear. The present study demonstrated that YY-20394 could inhibit cell viability in MV-4-11, THP-1 and U937 cells, consistent with the effects of other PI3Kδ inhibitors (29,30). Although U937 cells exhibited the lowest sensitivity, YY-20394 suppressed their proliferation, promoted apoptosis, and induced G_1/S and early S phase arrest in a concentration-dependent manner. These effects contribute to its antitumor activity in AML cells.

Due to the issue of acquired resistance to ABT199, it is often not recommended as a monotherapy for AML (20). The present findings demonstrate that the combination of YY-20394 and ABT199 exerts synergistic effects in MV-4-11 cells, reducing cell survival and enhancing apoptosis more effectively than either agent alone. MV-4-11 cells are an AML cell line positive for FLT3-ITDs, a common driver mutation associated with poor prognosis and present in ~25% of AML cases (31,32). While ABT199 monotherapy has limited efficacy in FLT3-ITD-mutated AML (33), the combination of ABT199 and PI3Kδ inhibitors has shown promise in preclinical studies (21,34). The present study supports previous research, suggesting that FLT3-ITD status may be associated with increased sensitivity to this combination strategy. Due to clonal variability among different FLT3-ITD-positive AML cell lines, the broader applicability of these findings should be further validated in additional models, such as MOLM-13 and MOLM-14.

Changes in apoptosis-related molecules were explored following treatment with YY-20394 and ABT199. The results

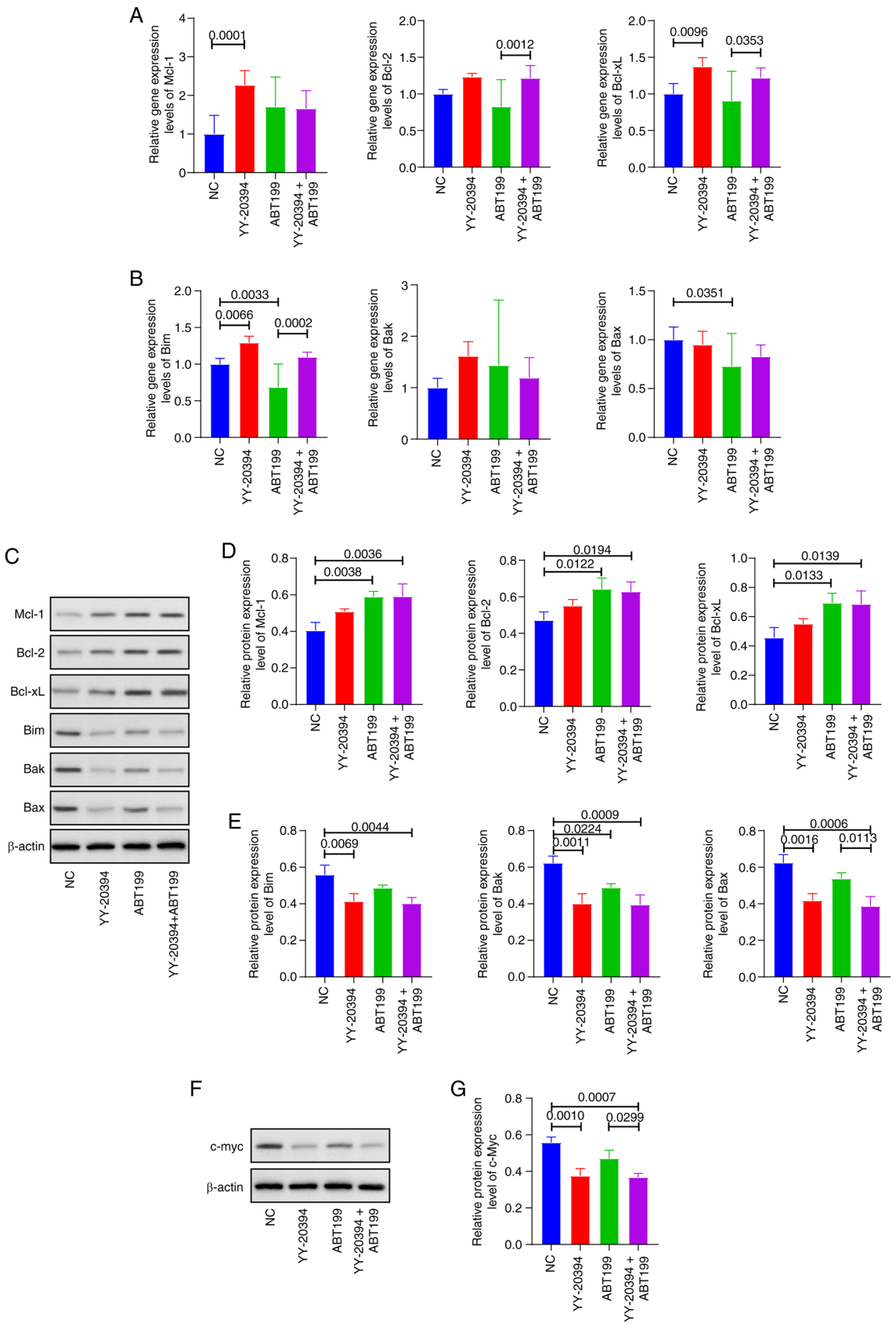

Figure 5. Effect of YY-20394 and ABT199 on apoptotic pathways in MV-4-11 cells. MV-4-11 cells were treated with 120 nM of ABT199, 30 nM of YY-20394 or a combination of both for 48 h. (A) The mRNA levels of anti-apoptotic factors Mcl-1, Bcl-2 and Bcl-xL were assessed using RT-qPCR. (B) The mRNA levels of pro-apoptotic factors Bim, Bak and Bax were assessed using RT-qPCR. (C) The protein results of Mcl-1, Bcl-2, Bcl-xL, Bim, Bak and Bax were assessed using western blotting. (D) The protein levels of Mcl-1, Bcl-2, and Bcl-xL were semi-quantified using densitometric analysis. (E) The protein levels of Bim, Bak and Bax were semi-quantified using densitometric analysis. (F) The protein results of c-Myc were assessed using western blotting and (G) the statistical result of densitometric analysis. Data are presented as mean ± SD from three independent experiments. RT-qPCR, reverse transcription-quantitative PCR; Mcl-1, myeloid cell leukemia-1; Bim, Bcl-2 interacting mediator of cell death; Bcl-xL, B-cell lymphoma-extra large; Bak, Bcl-2 antagonist killer 1; Bax, Bcl-2 associated X.

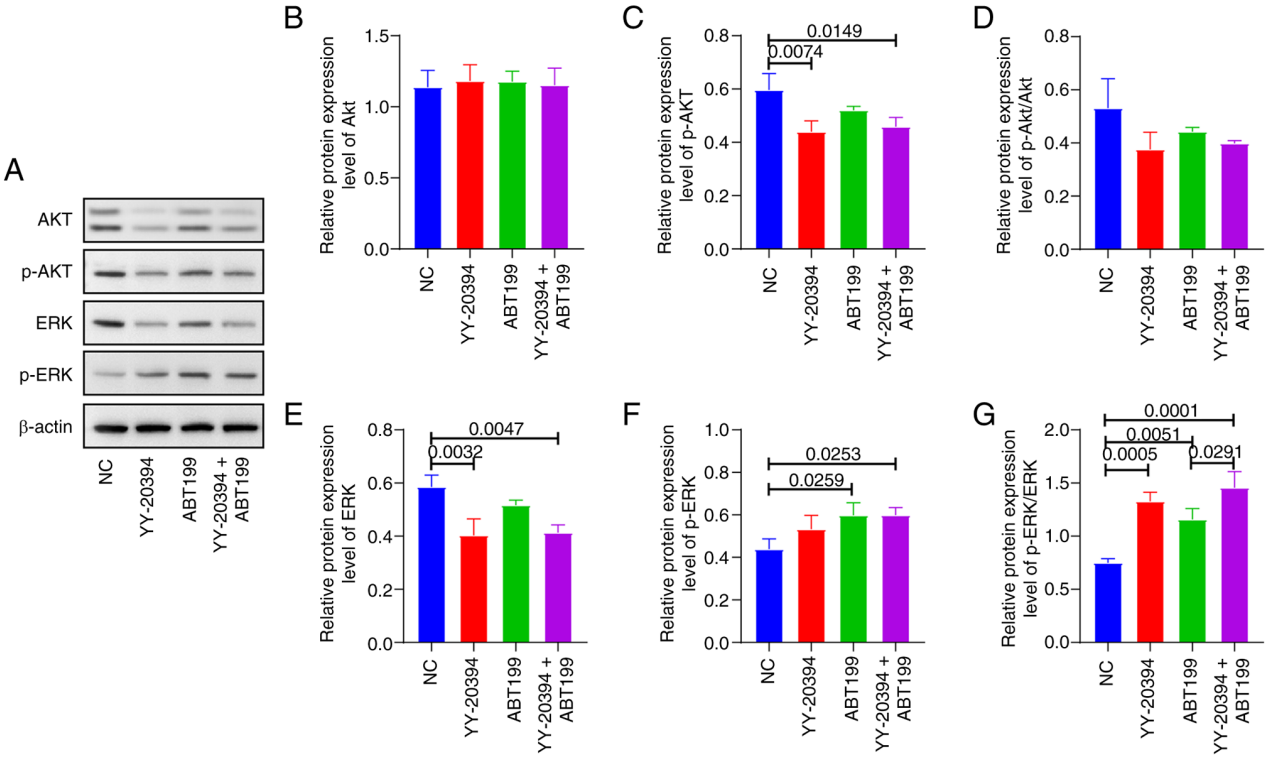

Figure 6. Effect of YY-20394 and ABT199 on p-AKT and p-ERK signaling pathways in MV-4-11 cells. MV-4-11 cells were treated with 120 nM of ABT199, 30 nM of YY-20394 or a combination of both for 48 h. (A) The protein levels of AKT, p-AKT (Ser473), ERK and p-ERK (Thr202/Tyr204) were examined using western blot. Densitometric analysis of western blot of (B) AKT, (C) p-AKT, (D) p-AKT/AKT, (E) ERK, (F) p-ERK and (G) p-ERK/ERK. Data are presented as mean ± SD from three independent experiments. p-, phosphorylated.

showed inconsistent changes between the transcriptional and protein levels of several apoptosis-related molecules in the combination group, suggesting the involvement of post-transcriptional regulation (35). For example, A-1210477 has been reported to disrupt the Mcl-1-Bim complex while stabilizing Mcl-1 protein, thereby promoting Mcl-1 accumulation independently of transcription (36). Consistent with the findings of Yao *et al* (21), inhibition of Bcl-2 or Bcl-xL by either ABT199 alone or in combination was not observed. Instead, significantly increased protein levels of Mcl-1, Bcl-2 and Bcl-xL were observed. ABT199 primarily functions as a BH3 mimetic that binds to Bcl-2 and inhibits its functional activity, rather than reducing its transcription or protein abundance. One possible explanation for this increase is activation of compensatory survival signaling pathways in parallel cascades (37,38), which may be associated with the increased p-ERK protein levels observed in the present study. A previous study has shown that ABT199 can induce compensatory activation of ERK1/2 and subsequently promote downstream Mcl-1 expression, a phenomenon frequently observed in FLT3-ITD AML cells (39). Meanwhile, PI3K inhibition has also been reported to induce compensatory ERK activation through the RAS/RAF/MEK/ERK pathway (38). ERK activation has been shown to maintain cellular homeostasis by regulating cell cycle-associated pathways (such as cyclin D1) and promoting anti-apoptotic signaling (such as Mcl-1) (40). Previous research showed that such adaptive signaling may enable cancer cells to tolerate therapeutic stress and potentially contribute to treatment resistance (41). Therefore, future studies could explore whether MEK or ERK inhibition may further enhance the synergistic pro-apoptotic effects of YY-20394 and ABT199.

In addition, although the transcriptional levels of the pro-apoptotic proteins Bim, Bak and Bax did not change significantly in the combination group, their protein levels were markedly decreased. We hypothesize that there may be two possible explanations. First, Bax and Bak are terminal effectors of mitochondrial apoptosis, and the reduction in total protein levels may reflect extensive apoptosis (42). Further studies are needed to investigate the expression of other BH3-only proteins (such as p53 upregulated modulator of apoptosis and phorbol-12-myristate-13-acetate-induced protein 1), as well as to assess Bax/Bak conformational changes or mitochondrial translocation to determine whether this decrease is secondary to apoptosis activation. Second, alternative cell death-related mechanisms may also contribute to this effect, including stress-induced apoptosis such as endoplasmic reticulum stress, caspase-independent apoptosis mediated by AIF and Endo G, death receptor-mediated extrinsic apoptosis, or even non-apoptotic programmed cell death pathways such as necroptosis (43).

c-Myc is known to be highly expressed in AML and is associated with poor prognosis and therapeutic resistance (44,45). Downregulation of c-Myc has been shown to enhance the activity of ABT199 more effectively than Mcl-1 inhibition (46). Compared with treatment with the PI3K/HDAC inhibitor CUDC-907 alone, its combination with ABT-199 did not result in further downregulation of c-Myc (47,48). Nevertheless, c-Myc served a critical role in the synergistic effect of CUDC-907 and ABT-199, as the combination caused marked

dysregulation of MYC target genes, which may contribute to AML cell apoptosis through regulation of mitochondrial function and induction of DNA damage. Consistent with the present results, the PI3K/HDAC inhibitor CUDC-907 synergistically induces apoptosis in AML cells in combination with ABT199, partially through c-Myc inhibition (47). Furthermore, preclinical research has reported that FLT3-ITD can specifically activate c-Myc through the PI3K/Akt signaling pathway (49). Based on these findings, the combinatory effects of YY-20394 and ABT199 may be linked to c-Myc downregulation.

Studies have suggested that the *in vitro* potency of drugs for hematological malignancies is more comparable to the average clinical exposure concentration (C-unbound, average), and such direct comparisons may better reflect clinical translational potential than other cancers (50). Pharmacokinetic studies in B cell malignancies have shown that both single-dose (20-140 mg) and multiple-dose (20-200 mg) administration of YY-20394 resulted in dose-dependent increases in drug exposure parameters [such as C_{max}, area under the curve $(AUC)_{0-t}$ and $AUC_{0-\infty}$] (11). For ABT199, the reported C_{max} under the standard 400 mg QD regimen is ~2.1 μg/ml (51). However, although higher drug exposure is generally associated with improved clinical response, it may also increase the risk of adverse events (52). Consistent with previous reports, the present results demonstrated substantial heterogeneity in ABT199 sensitivity among different AML cell lines (17,53). However, due to the clinically achievable unbound drug exposure, the relatively high IC_{50} values observed in U937 and THP-1 cells may suggest limited efficacy of YY-20394 or ABT199 monotherapy in these clinical subtypes (54). Notably, the 48 h IC_{50} values were 2-10-fold lower than those at 24 h, indicating that prolonged drug exposure may enhance antileukemic activity. Therefore, optimization of dosing schedules to maintain effective exposure may help broaden the therapeutic window and improve translational potential.

The present study has several limitations. First, all experiments were conducted *in vitro* using a limited panel of AML cell lines, which may not fully reflect the biological heterogeneity of AML in patients. Second, the mechanistic findings regarding the involvement of the c-Myc/Akt and ERK pathways are primarily correlative and require further functional validation. The precise contribution of Bcl-2 family proteins to the synergistic pro-apoptotic effects remains incompletely understood. Further studies are needed to investigate the functional status of these proteins, including their conformational activation, mitochondrial translocation and post-translational modifications. Fourth, no *in vivo* studies or primary patient-derived AML samples were included to evaluate the therapeutic efficacy and translational relevance of YY-20394 alone or in combination with ABT199. Future studies incorporating animal models, primary AML samples and more comprehensive mechanistic investigations will be necessary to further validate and extend the present findings.

An emerging strategy to enhance the therapeutic index of targeted agents in AML is nanocarrier based delivery. Nanoparticle formulations can improve pharmacokinetics, enable co-delivery of synergistic drug pairs, enhance tumor/bone marrow targeting and reduce off-target hematologic toxicity. Recent advances in nanoparticle design, including zein-based carriers for *in vivo* antitumor delivery (55), antibody functionalized lipid nanocarriers for targeted RNA/drug delivery (56) and next-generation lipid nanocarriers enabling novel administration routes (57), illustrate the translational potential of these platforms. In the context of YY-20394 and venetoclax, a nanocarrier approach could allow lower systemic doses while maintaining effective intratumoral concentrations, facilitate synchronized drug exposure and potentially overcome microenvironment mediated resistance. Preclinical evaluation of such co-delivery formulations in FLT3 ITD AML models would therefore be a promising translational step.

In conclusion, YY-20394 exhibits potential growth-inhibitory effects across different AML cell lines, making it a promising therapeutic candidate for AML. Moreover, the combination of YY-20394 and ABT199 demonstrates synergistic antitumor activity in MV-4-11 cells.

Acknowledgements

Not applicable.

Funding

The present work was supported by the Health Research Program of Anhui (grant no. AHWJ2023BAc10019 to YG).

Availability of data and materials

The data generated in the present study may be requested from the corresponding author.

Authors' contributions

YG, WW and YY conceived of and designed the study, contributed to manuscript drafting and revised the manuscript. JC and YL collected and curated data. LZ, QL and JS provided materials and samples. YG, LZ, QL and JS performed analysis and interpretation of data and conducted statistical analysis. WW and YY confirm the authenticity of all raw data. All authors read and approved the final version of the manuscript.

Ethics approval and consent to participate

Not applicable.

Patient consent for publication

Not applicable.

Competing interests

The authors declare that they have no competing interests.

References

1. DiNardo CD, Erba HP, Freeman SD and Wei AH: Acute myeloid leukaemia. Lancet 401: 2073-2086, 2023.
2. Juliusson G, Hagberg O, Lazarevic VL, Ölander E, Antunovic P, Cammenga J, Wennström L, Möllgård L, Brune M, Jädersten M, *et al*: Improved survival of men 50 to 75 years old with acute myeloid leukemia over a 20-year period. Blood 134: 1558-1561, 2019.

3. Song Y, Jia Y, Zhang G, Wei S, Li Y, Hu Y, Hao Q, Wang Z, Fang Q, Tian Z, *et al*: Machine leaning algorithm on chemotherapeutic drug resistance related gene classifier in acute myeloid leukemia. Blood 136: 28-29, 2020.
4. Ma YR, Zhao T, Ma L, Hu LJ, Duan WB, Jiang H, Huang XJ and Jiang Q: Variables associated with hematological remission and survival in patients with acute myeloid leukemia after induction failure and relapse. Zhonghua Xue Ye Xue Za Zhi 43: 644-650, 2022 (In Chinese).
5. Wysota M, Konopleva M and Mitchell S: Novel therapeutic targets in acute myeloid leukemia (AML). Curr Oncol Rep 26: 409-420, 2024.
6. Bazinet A and Kantarjian HM: Moving toward individualized target-based therapies in acute myeloid leukemia. Ann Oncol 34: 141-151, 2023.
7. Nepstad I, Hatfield KJ, Grønningsæter IS and Reikvam H: The PI3K-Akt-mTOR signaling pathway in human acute myeloid leukemia (AML) cells. Int J Mol Sci 21: 2907, 2020.
8. Feng Y, Cu X and Xin M: PI3Kδ inhibitors for the treatment of cancer: A patent review (2015-present). Expert Opin Ther Pat 29: 925-941, 2019.
9. Tang Y, Zheng Y, Hu X, Zhao H and Cui S: Discovery of potent and selective PI3Kδ inhibitors for the treatment of acute myeloid leukemia. J Med Chem 67: 6638-6657, 2024.
10. Liang X, Li F, Chen C, Jiang Z, Wang A, Liu X, Ge J, Hu Z, Yu K, Wang W, *et al*: Discovery of (S)-2-amino-N-(5-(6-chloro-5-(3-methylphenylsulfonamido)pyridin-3-yl)-4-methylthiazol-2-yl)-3-methylbutanamide (CHMFL-PI3KD-317) as a potent and selective phosphoinositide 3-kinase delta (PI3Kδ) inhibitor. Eur J Med Chem 156: 831-846, 2018.
11. Jiang B, Qi J, Song Y, Li Z, Tu M, Ping L, Liu Z, Bao H, Xu Z and Qiu L: Phase 1 clinical trial of the PI3Kδ inhibitor YY-20394 in patients with B-cell hematological malignancies. J Hematol Oncol 14: 130, 2021.
12. Jin J, Cen H, Zhou K, Xu X, Li F, Wu T, Yang H, Wang Z, Li Z, Huang W, *et al*: A Phase Ib study of linperlisib in the treatment of patients with relapsed and/or refractory peripheral T-cell lymphoma. Clin Cancer Res 30: 4593-4600, 2024.
13. Wang T, Sun X, Qiu L, Su H, Cao J, Li Z, Song Y, Zhang L, Li D, Wu H, *et al*: The oral PI3Kδ inhibitor linperlisib for the treatment of relapsed and/or refractory follicular lymphoma: A phase II, Single-Arm, Open-label clinical trial. Clin Cancer Res 29: 1440-1449, 2023.
14. Wu J, Lu AD, Zhang LP, Zuo YX and Jia YP: Study of clinical outcome and prognosis in pediatric core binding factor-acute myeloid leukemia. Zhonghua Xue Ye Xue Za Zhi 40: 52-57, 2019 (In Chinese).
15. Wu D, Li M, Hong Y, Jin L, Liu Q, Sun C, Li L, Han X, Deng S, Feng Y, *et al*: Integrated stress response activation induced by usnic acid alleviates BCL-2 inhibitor ABT-199 resistance in acute myeloid leukemia. J Adv Res 74: 621-635, 2025.
16. Liu J, Chen Y, Yu L and Yang L: Mechanisms of venetoclax resistance and solutions. Front Oncol 12: 1005659, 2022.
17. Liu H, Hussain Z, Xie Q, Yan X, Zeng C, Zhou G and Cao S: Targeting PI3K/AKT/mTOR pathway to enhance the anti-leukemia efficacy of venetoclax. Exp Cell Res 417: 113192, 2022.
18. Zhang K, Huang Y, Duan Y, Guo B, Ke Q, Liao C and Cen H: Anti-tumor effect of PI3K inhibitor Linperlisib on diffuse large B-cell lymphoma in vitro. Chin J Oncol Prev Treat 16: 56-61, 2024 (In Chinese).
19. Alkhatabi HA, Zohny SF, Shait Mohammed MR, Choudhry H, Rehan M, Ahmad A, Ahmed F and Khan MI: Venetoclax-resistant MV4-11 leukemic cells activate PI3K/AKT pathway for metabolic reprogramming and redox adaptation for survival. Antioxidants (Basel) 11: 461, 2022.
20. Ren WX, Guo H, Lin SY, Chen SY, Long YY, Xu LY, Wu D, Cao YL, Qu J, Yang BL, *et al*: Targeting cytohesin-1 suppresses acute myeloid leukemia progression and overcomes resistance to ABT-199. Acta Pharmacol Sin 45: 180-192, 2024.
21. Yao MY, Wang YF, Zhao Y, Ling LJ, He Y, Wen J, Zheng MY, Jiang HL and Xie CY: BCL-2 inhibitor synergizes with PI3Kδ inhibitor and overcomes FLT3 inhibitor resistance in acute myeloid leukaemia. Am J Cancer Res 12: 3829-3842, 2022.
22. Livak KJ and Schmittgen TD: Analysis of relative gene expression data using real-time quantitative PCR and the 2(-Delta Delta C(T)) method. Methods 25: 402-408, 2001.
23. Vela L, Gonzalo O, Naval J and Marzo I: Direct interaction of Bax and Bak proteins with Bcl-2 homology domain 3 (BH3)-only proteins in living cells revealed by fluorescence complementation. J Biol Chem 288: 4935-4946, 2013.
24. Zhao J, Wu S, Wang D, Edwards H, Thibodeau J, Kim S, Stemmer P, Wang G, Jin J, Savasan S, *et al*: Panobinostat sensitizes AraC-resistant AML cells to the combination of azacitidine and venetoclax. Biochem Pharmacol 228: 116065, 2024.
25. Wang X, Zhang X, Li BS, Zhai X, Yang Z, Ding LX, Wang H, Liang C, Zhu W, Ding J and Meng LH: Simultaneous targeting of PI3Kδ and a PI3Kδ-dependent MEK1/2-Erk1/2 pathway for therapy in pediatric B-cell acute lymphoblastic leukemia. Oncotarget 5: 10732-10744, 2014.
26. Xie C, He Y, Zhen M, Wang Y, Xu Y and Lou L: Puquitinib, a novel orally available PI3Kδ inhibitor, exhibits potent antitumor efficacy against acute myeloid leukemia. Cancer Sci 108: 1476-1484, 2017.
27. Xiang Q, Dong S and Li XH: A Review of phosphocreatine 3 kinase δ subtype (PI3Kδ) and its inhibitors in malignancy. Med Sci Monit 27: e932772, 2021.
28. Zou L, Qi Y, Tang L, Du Y, Xiang M, Chen X, Ma J and Yang Z: Clinical review considerations of class I PI3K inhibitors in hematolymphatic malignancies by Center for Drug Evaluation. Chin J Cancer Res 34: 415-421, 2022.
29. Chen Y, Wu T, Yang C, Lu M, Chen Z, Deng M, Jia Y, Yang Y, Liu X, Wang H, *et al*: A pyridinesulfonamide derivative FD268 suppresses cell proliferation and induces apoptosis via inhibiting PI3K pathway in acute myeloid leukemia. PLoS One 17: e0277893, 2022.
30. Yang C, Gong Y, Gao Y, Deng M, Liu X, Yang Y, Ling Y, Jia Y and Zhou Y: Design, synthesis and in vitro biological evaluation of 2-aminopyridine derivatives as novel PI3Kδ inhibitors for hematological cancer. Bioorg Med Chem Lett 82: 129152, 2023.
31. Song G, Valdez BC, Li Y, Liu Y, Champlin RE and Andersson BS: Synergistic cytotoxicity of sorafenib with busulfan and nucleoside analogs in human FMS-like tyrosine kinase 3 internal tandem duplications-positive acute myeloid leukemia cells. Biol Blood Marrow Transplant 20: 1687-1695, 2014.
32. Daver N, Schlenk RF, Russell NH and Levis MJ: Targeting FLT3 mutations in AML: Review of current knowledge and evidence. Leukemia 33: 299-312, 2019.
33. Konopleva M, Pollyea DA, Potluri J, Chyla B, Hogdal L, Busman T, McKeegan E, Salem AH, Zhu M, Ricker JL, *et al*: Efficacy and biological correlates of response in a phase II study of venetoclax monotherapy in patients with acute myelogenous leukemia. Cancer Discov 6: 1106-1117, 2016.
34. Darici S, Alkhaldi H, Horne G, Jørgensen HG, Marmiroli S and Huang X: Targeting PI3K/Akt/mTOR in AML: Rationale and clinical evidence. J Clin Med 9: 2934, 2020.
35. Cui J and Placzek WJ: Post-Transcriptional regulation of Anti-apoptotic BCL2 family members. Int J Mol Sci 19: 308, 2018.
36. Leverson JD, Zhang H, Chen J, Tahir SK, Phillips DC, Xue J, Nimmer P, Jin S, Smith M, Xiao Y, *et al*: Potent and selective small-molecule MCL-1 inhibitors demonstrate on-target cancer cell killing activity as single agents and in combination with ABT-263 (navitoclax). Cell Death Dis 6: e1590, 2015.
37. Piddock RE, Bowles KM and Rushworth SA: The role of PI3K isoforms in regulating bone marrow microenvironment signaling focusing on acute myeloid leukemia and multiple myeloma. Cancers (Basel) 9: 29, 2017.
38. Serra V, Scaltriti M, Prudkin L, Eichhorn PJ, Ibrahim YH, Chandarlapaty S, Markman B, Rodriguez O, Guzman M, Rodriguez S, *et al*: PI3K inhibition results in enhanced HER signaling and acquired ERK dependency in HER2-overexpressing breast cancer. Oncogene 30: 2547-2557, 2011.
39. Kiyoi H, Kawashima N and Ishikawa Y: FLT3 mutations in acute myeloid leukemia: Therapeutic paradigm beyond inhibitor development. Cancer Sci 111: 312-322, 2020.
40. Lu Y, Liu B, Liu Y, Yu X and Cheng G: Dual effects of active ERK in cancer: A potential target for enhancing radiosensitivity (Review). Oncol Lett 20: 993-1000, 2020.
41. Ondrisova L and Mraz M: Genetic and Non-Genetic mechanisms of resistance to BCR signaling inhibitors in B cell malignancies. Front Oncol 10: 591577, 2020.
42. Wolf P, Schoeniger A and Edlich F: Pro-apoptotic complexes of BAX and BAK on the outer mitochondrial membrane. Biochim Biophys Acta Mol Cell Res 1869: 119317, 2022.
43. Mustafa M, Ahmad R, Tantry IQ, Ahmad W, Siddiqui S, Alam M, Abbas K, Moinuddin, Hassan MI, Habib S and Islam S: Apoptosis: A comprehensive overview of signaling pathways, morphological changes, and physiological significance and therapeutic implications. Cells 13: 1838, 2024.

44. Ohanian M, Rozovski U, Kanagal-Shamanna R, Abruzzo LV, Loghavi S, Kadia T, Futreal A, Bhalla K, Zuo Z, Huh YO, *et al*: MYC protein expression is an important prognostic factor in acute myeloid leukemia. Leuk Lymphoma 60: 37-48, 2019.
45. Gu K, May HA and Kang MH: Targeting molecular signaling pathways and cytokine responses to modulate c-MYC in acute myeloid leukemia. Front Biosci (Schol Ed) 16: 15, 2024.
46. Carter JL, Hege K, Yang J, Kalpage HA, Su Y, Edwards H, Hüttemann M, Taub JW and Ge Y: Targeting multiple signaling pathways: The new approach to acute myeloid leukemia therapy. Signal Transduct Target Ther 5: 288, 2020.
47. Hege Hurrish K, Qiao X, Li X, Su Y, Carter J, Ma J, Kalpage HA, Hüttemann M, Edwards H, Wang G, *et al*: Co-targeting of HDAC, PI3K, and Bcl-2 results in metabolic and transcriptional reprogramming and decreased mitochondrial function in acute myeloid leukemia. Biochem Pharmacol 205: 115283, 2022.
48. Li X, Su Y, Hege K, Madlambayan G, Edwards H, Knight T, Polin L, Kushner J, Dzinic SH, White K, *et al*: The HDAC and PI3K dual inhibitor CUDC-907 synergistically enhances the antileukemic activity of venetoclax in preclinical models of acute myeloid leukemia. Haematologica 106: 1262-1277, 2021.
49. Basit F, Andersson M and Hultquist A: The Myc/Max/Mxd network is a target of mutated Flt3 signaling in hematopoietic stem cells in Flt3-ITD-Induced myeloproliferative disease. Stem Cells Int 2018: 3286949, 2018.
50. Kotani N and Ito K: Translatability of in vitro potency to clinical efficacious exposure: A retrospective analysis of FDA-approved targeted small molecule oncology drugs. Clin Transl Sci 16: 1359-1368, 2023.
51. Salem AH and Menon RM: Clinical pharmacokinetics and pharmacodynamics of venetoclax, a selective B-cell lymphoma-2 inhibitor. Clin Transl Sci 17: e13807, 2024.
52. Kobayashi T, Sato H, Miura M, Fukushi Y, Kuroki W, Ito F, Teshima K, Watanabe A, Fujishima N, Kobayashi I, *et al*: Overexposure to venetoclax is associated with prolonged-duration of neutropenia during venetoclax and azacitidine therapy in Japanese patients with acute myeloid leukemia. Cancer Chemother Pharmacol 94: 285-296, 2024.
53. Kuusanmäki H, Kytölä S, Vänttinen I, Ruokoranta T, Ranta A, Huuhtanen J, Suvela M, Parsons A, Holopainen A, Partanen A, *et al*: Ex vivo venetoclax sensitivity testing predicts treatment response in acute myeloid leukemia. Haematologica 108: 1768-1781, 2023.
54. Graham GG and Scott KF: Limitations of drug concentrations used in cell culture studies for understanding clinical responses of NSAIDs. Inflammopharmacology 29: 1261-1278, 2021.
55. Abosalim HM, El-Moselhy TF, Sharafeldin N, Giovannuzzi S, Begines P, Nafie MS, Fahmy SA, Diab MK, Babker A, Supuran CT, *et al*: Innovative design and synthesis of dual-acting hCA IX/CDK-2 inhibitors through hetero ring fused pyrimidine utilization for cutting-edge anticancer therapy: Zein nanoparticles for in vivo lung cancer treatment. Bioorg Chem 166: 109057, 2025.
56. Nabih NW, Hassan H, Preis E, Schaefer J, Babker A, Abbas AM, Amin MU, Bakowsky U and Fahmy SA: Antibody-functionalized lipid nanocarriers for RNA-based cancer gene therapy: Advances and challenges in targeted delivery. Nanoscale Adv 7: 5905-5931, 2025.
57. Wafik Nabih N, Nafie MS, Babker A, Alameen AAM and Fahmy SA: Next-generation lipid nanocarriers for Parkinson's therapy: Nose-to-brain innovations and clinical prospects. Nanoscale 17: 27826-27848, 2025.